20th European Photovoltaic Solar Energy Conference and Exhibition, Barcelona, 6-10 June 2005
Pre-Print, 2DV2.49

INVESTIGATION OF THE ALLOYING PROCESS OF SCREEN PRINTED ALUMINIUM PASTES FOR THE BSF FORMATION ON SILICON SOLAR CELLS

F. Huster
University of Konstanz, Department of Physics, 78457 Konstanz, Germany
email: frank.huster@uni-konstanz.de

ABSTRACT: This paper is intended to give insights into the formation process of aluminium alloyed back surface fields (BSF) and rear contacts made by firing screen printed aluminium pastes. It is shown that a sufficient oxygen supply from the gas ambient is important to thicken and strengthen the oxide shells enclosing the liquid aluminium and silicon during firing. The alloying action of the aluminium from the paste particles and the silicon of the wafer surface is starting locally at points where they are in an intimate contact. To achieve a closed BSF it is necessary to have a closed liquid Al-Si layer on the surface at T_{peak}, usually requiring a minimum of 6 mg/cm^2 deposited amount of aluminium. Larger amounts of aluminium (>10 mg/cm^2) are only incompletely used for the BSF formation. After firing there is always a thin but compact layer of eutectic aluminium – silicon present between the BSF surface and the paste particles. This layer determines the internal reflectivity which is calculated to nearly 80% in accordance with recent publications.
Keywords: Aluminium, Back Surface Field, Screen Printing

1 INTRODUCTION

The formation on an alloyed aluminium back surface field (BSF) made from firing a screen printed paste is an important part of current processes for the vast majority of silicon solar cell production. Despite this importance and the long lasting research on the Al BSF over three decades some interesting details about the formation process and the resulting structure are not common knowledge today. This paper aims to provide new insights about the BSF formation in an industrial cell process and thereby to serve as a basis for the understanding and optimization or control of the important BSF properties like doping profile and BSF thickness (→ passivation properties), wafer bow, rear surface reflectivity and BSF homogeneity.
The experiments were carried out using mainly the commercial Al-paste Ferro 53-038 (fritted) on (100) oriented silicon substrates, fired in an RTP furnace with a close temperature and gas composition control.

2 BSF FORMATION

Usually the aluminium BSF is formed in the contact firing step of an industrial type solar cell process. A typical temperature profile for firing the front contact through a SiN_x layer in a belt furnace is shown in fig. 1.

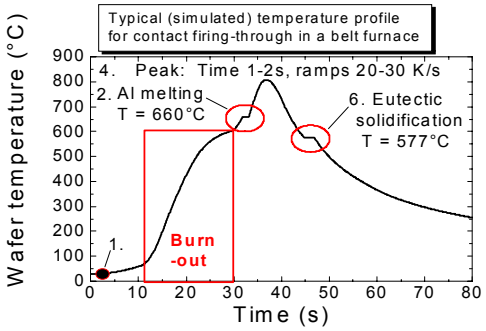

Figure 1: Temperature profile for firing through a silicon nitride layer in a belt furnace. After the burn out of the organic components (binders) the front contact and at the same time the BSF and rear contact are formed in the peak firing step ("co-firing", between 2. and 6.).

According to the binary phase diagram (see figure 2) of aluminium and silicon a liquid phase is formed at the solar cell rear surface, from which on cooling down the BSF is formed. The details of this process are described below:

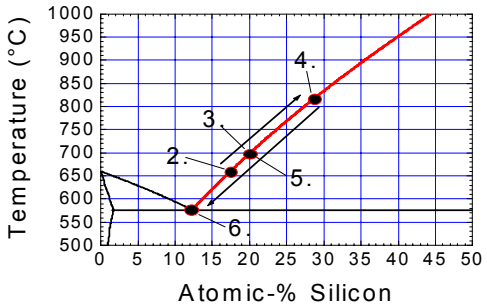

Figure 2: Calculated binary phase diagram of aluminium and silicon, see for instance [1]

Description of the BSF formation process according to the numbers 1.-6. in figures 1 – 3:

1. The aluminium paste consists of aluminium particles of 1 to 10 µm diameter, a glass frit to enhance sintering, organic binders and solvents. After drying (removal of solvents) a porous paste matrix with a filling of 50 to 70 % is attached to the surface by the binders. A typical amount of aluminium deposition is 6 to 7 mg/cm^2 (40 µm thickness).
2. After the burn-out of the organic binders the peak firing zone is entered. The alloying process starts with the melting of the aluminium at 660°C which can be seen in a small temperature plateau of measured profiles (latent heat). The liquid aluminium is able to penetrate locally the native oxide shells of the Al particles to make contact: 1. to the silicon surface to start the alloying with silicon, and 2. to neighbouring Al particles. Two important points have to be emphasized:
   a. The alloying reaction starts LOCALLY on the wafer surface; no full coverage of the surface by liquid aluminium is reached at that time.
   b. The native oxide shells are thickened during firing to stabilize the paste matrix (see next section). The paste particles are hold in place during the whole firing process [2]. The transport

of the liquid phase containing Al and Si takes place within these oxide shells, from particle to particle via small sintering necks.

3. Soon after Al melting the composition of ALL paste particles assume the thermodynamic equilibrium according to the binary phase diagram. On further heating up more and more silicon is dissolved in the liquid phase. The volume of the particles is kept constant, confined by the oxide shells. To compensate for the additional silicon which is incorporated into the particles the same volume of aluminium is transported towards the wafer surface. This matter transport (On heating up: silicon from the wafer surface towards the outer paste layers, and aluminium towards wafer surface. On cooling down: reverse procedure) is obviously very fast and complete, at least for a moderate Al layer thickness, see also section 5.
4. At the peak temperature almost 30% of the liquid phase consists of silicon. As the processes of dissolving silicon and transportation of the liquid phases are very fast, fast ramps and short dwell times at peak temperature (1 s is sufficient, except for special configurations) can be applied. On the wafer surface there is a "lake" of liquid Al-Si with exactly the same volume as that of the dissolved silicon. From this lake the BSF is subsequently grown epitaxially. For achieving a closed BSF it is necessary to have a full coverage of the rear surface by this lake, see section 6.
5. On cooling down the fast matter transport of step 3 is reversed: Going down on the liquidus curve of the phase diagram, silicon is rejected from the melt to recrystallize epitaxially on the wafer surface, building up the BSF. At the same time aluminium is incorporated into the silicon lattice according to the temperature dependent solid solubility.
6. After reaching the eutectic temperature of 577°C (usually some degrees below due to undercooling) the remaining liquid phase solidifies within a second (2nd temperature plateau in the firing profile). Because in the paste particles there is now Al-Si of nearly eutectic composition (approx. 12% silicon) instead of pure aluminium as before, a certain amount of aluminium is found on the wafer surface. Therefore an Al-Si layer of a compact structure is always present after firing on the BSF surface (see section 4).

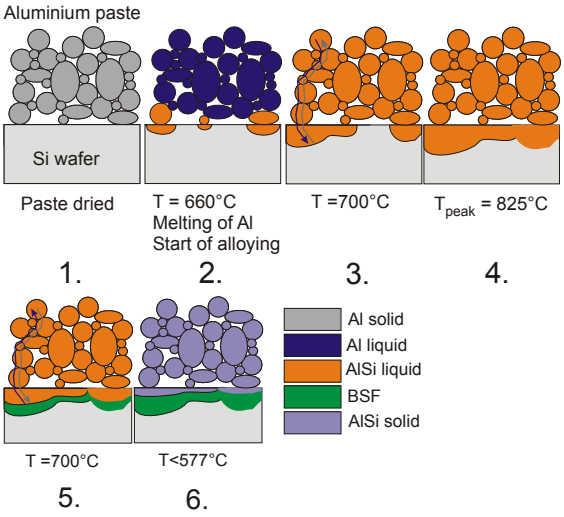

Figure 3: Formation of the aluminium back surface field and rear contact from a screen printed aluminium paste.

3 OXIDE SHELLS

The thin native oxide on the paste aluminium particles is thickened during firing by oxidation at the elevated temperatures. These Al_2O_3 shells provide a stable structure, holding the particles in place as it is observable by taking SEM pictures of the paste after drying (figure 4a) and after firing (4b) at the same sites. EDX measurements confirmed the composition to be mainly Al after drying and Al, Si and O in the expected concentration range after firing[1]. A slight densification is visible. Large Al particles tend to collapse and empty their liquid content to the wafer surface.

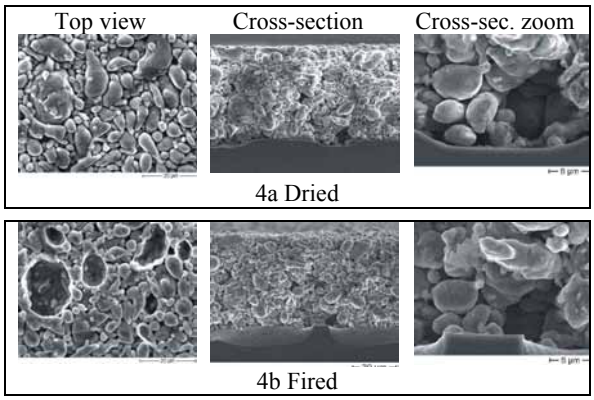

Figure 4: SEM pictures of a screen printed aluminium paste before and after firing.

3.2 Thickness of oxide shells

The native oxide on aluminium particles has a thickness of about 1 nm. From SEM pictures of emptied aluminium particles (figure 5) the final oxide thickness after firing can be estimated to roughly 100 - 200 nm. This is in good agreement with a thickness determination which is done simply by weighing: The paste weight is measured after the burn-out of the organic components and after firing. Indeed a mass increase was measured, which is interpreted as the oxidation of parts of the aluminium to Al_2O_3. In a typical firing sequence in air ambient about 1% of the total amount of aluminium is oxidized, which corresponds to an oxide shell thickness of 100 nm assuming an Al particle diameter of 5 µm.

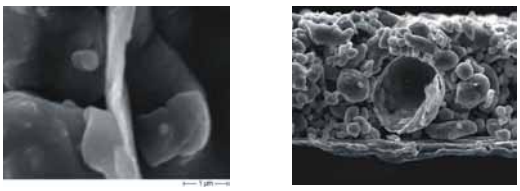

Figure 5: SEM pictures of collapsed Al particles, exposing the thin oxide skins (after firing). The picture on the left was taking with 25000x magnification showing an Al_2O_3 wall of 100 – 200 nm thickness.

3.2 Gas ambient

The importance of a sufficient oxygen supply in the gas ambient during firing can be demonstrated by firing in an inert atmosphere (N_2): The paste matrix becomes unstable and is collapsing. In figure 6 the resulting paste islands can be clearly seen.

[1] Quantitative EDX results are difficult to achieve due to the uneven surface of the small particles.

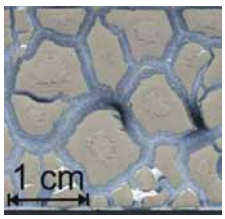

Figure 6: Aluminium rear contact after firing in an inert gas ambient (N_2).

If on the other side the firing is done in a pure oxygen atmosphere, the oxidation of the aluminium occurs in an explosive (or more correctly: implosive) reaction, leading to wafer destruction.

4 AL – SI INTERFACE LAYER

4.1 Description

After firing there is always a compact Al-Si layer present between the BSF and the paste matrix. It is of nearly eutectic composition, exhibiting the well-known lamella structure of silicon in aluminium. The outer surface of this layer coincides with the former silicon wafer surface. Sometimes large cavities are found in this layer (see figure 7 on the left), whose origin is not clear. The thickness of the Al-Si layer is determined by the amount of silicon which is incorporated in the paste particles after firing, replacing some aluminium which is found in the Al-Si layer. A simple calculation leads to approx. 0.5 µm / (mg/cm^2 deposited Al), neglecting Al-Si from emptied, collapsed paste particles.

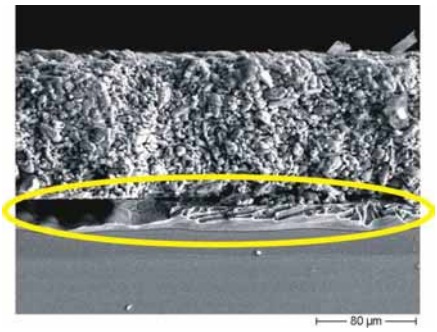

Figure 7: SEM cross-section of a fired Al rear contact (upside down). Between the BSF (dark gray layer below) and the paste matrix (above) the compact Al-Si layer is present. On the left side a cavity in the layer can be seen. The small holes in the remaining part contained Si lamellas before cleaving.

The Al-Si layer is important for two reasons:

1. The physical surface of the BSF is actually the interface of the BSF to the Al-Si-layer (aluminium with a very low content of silicon plus 12% silicon in lamella form). The internal rear surface reflectivity is determined by this interface, not by the porous paste matrix.
2. A wafer bow is caused by the strong contraction of the aluminium after firing. While the mechanical properties of the paste matrix are strongly influenced by the sintering conditions (particle size, frit content, firing conditions), the properties of the Al-Si layer are only depending on its thickness.

4.2 Silicon lamellas

The solidified Al-Si alloy of eutectic composition actually consists of two phases: an almost pure Al containing Si lamellas with a branch size and spacing of a few µm. This structure can be found on top of the Al-Si layer after carefully removing the paste matrix mechanically (figure 8 left). This is possible because the paste matrix is attached to the layer at only small points, where the paste particles were in contact with the silicon surface during firing.

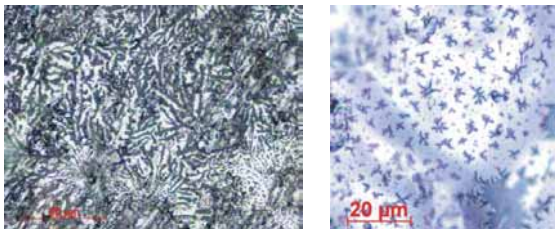

Figure 8: Optical microscope pictures of the silicon lamella structure in aluminium. Top views on the Al-Si layer, on the left: well known lamellas, on the right: to p view on the cavity, showing a star-like pattern instead of lamellas.

The silicon lamellas can be exposed by selectively removing the aluminium in cold HCl, see figure 9. The structures where the lamellas are attached to the BSF surface are probably important for the surface reflectivity.

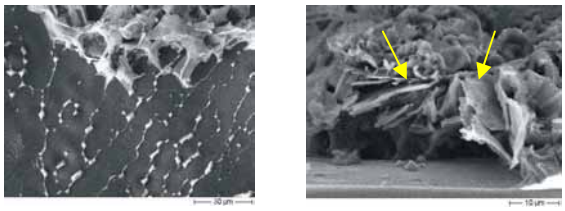

Top view. After removal of the brittle silicon lamellas small silicon structures are remaining on the surface.

Side view. The top surface of the removed Al-Si layer is indicated by the arrows.

Figure 9: SEM pictures of silicon lamellas after removal of the aluminium in HCl.

4.3 Model for Al-BSF rear surface reflectivity

The effective rear surface reflectivity of an alloyed Al-BSF is difficult to determine experimentally, but values between 75 and 80% are most probable [3]. Lower values published elsewhere might be the result of very rough surfaces and a non-closed BSF. According to the interface structure described above a new model to explain this reflectivity is proposed, comprising contributions by free carrier absorption in the BSF (5% per double ray transit, depending on BSF thickness, doping level and ray angle) and by the physical BSF surface. 90% of the surface is covered by aluminium (reflectivity Si-Al nearly 90% @ λ=1200nm) and 10% by silicon structures connected to the lamellas. Theses structures act as light traps and can be modelled with zero reflectivity. The total reflectivity then amounts to: 95% (FCA) * (0.9*90% (Si-Al) + 0.1*0% (lamella cavities)) = 77% effective reflectivity.

5 EFFECTIVENESS OF BSF FORMATION

As long as the alloying and BSF growth process is following the phase diagram the final BSF thickness can be easily calculated from the amount of deposited Al and the firing peak temperature. The thickness and the sheet resistance are proportional to the aluminium layer thickness. But if very thick aluminium layers are printed

a deviation from this linearity occurs, i.e. a saturation of the BSF thickness increase is observed at about 10 µm (depending on aluminium paste, crystal orientation and firing conditions). Two effects are responsible for this saturation: first, some of the aluminium in the outer paste layers is not entering the alloying reaction (Al content in these particles remain above 70%), and second, some of the silicon dissolved in the liquid aluminium is not transported fast enough towards the wafer surface for BSF growth (paste particles are hypereutectic after solidification). With the use of the phase diagram, the known peak temperature and weighing the solar cell after paste drying, after firing and after Al-Si removal in HCl these effects can be separated.

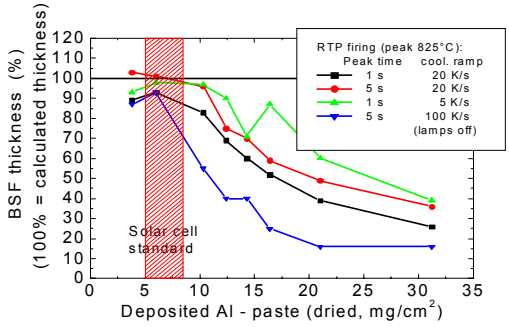

Figure 10a: BSF thickness vs. deposited Al thickness. 100% reference is calculated, assuming a linear dependence of BSF thickness on the amount of Al.

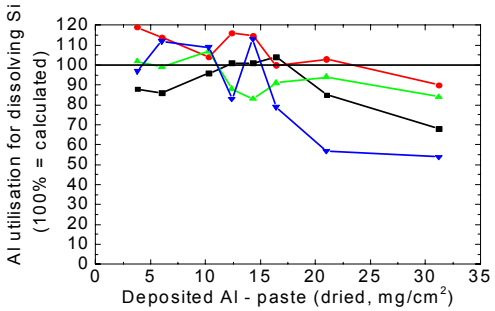

Figure 10b: Amount of aluminium taking part in the alloying process.

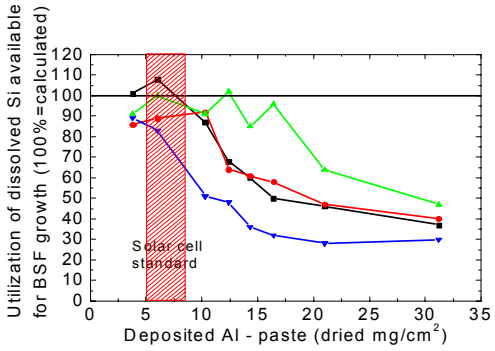

Figure 10c: Amount of dissolved silicon taking part in the epitaxial BSF growth.

The results given in figures 10a to 10c indicate that the bottleneck for achieving very thick BSF layers is the transport of the Si in liquid phase back to the regrowing BSF layer (fig. 10c). Firing more slowly (cool down ramp and dwell time) can diminish this effect but on the risk of an Al-Si agglomeration (see next section).

6 INHOMOGENEOUS BSF FORMATION

6.1 Insufficient Al deposition

If the amount of Al is too low, only a thin liquid Al-Si layer is formed. As the alloying process starts locally on the silicon surface, a non-closed BSF and a strongly increased surface recombination velocity results.

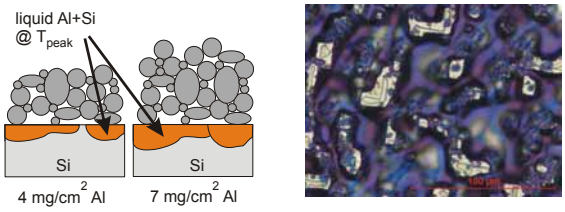

Figure 11: Thin aluminium layers might result in a non-closed BSF. On the right an optical microscope picture after Al-Si removal in HCl is shown. The BSF areas are colored for a better contrast.

6.2 Al-Si agglomeration

A high peak temperature (>850°C) in combination with a medium to large Al thickness leads to an agglomeration of the liquid Al/Si into islands. The BSF grown under the islands is thick but rough while a very thin BSF is present in the areas between [4].

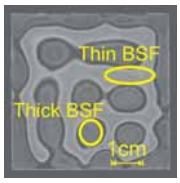

Figure 12: BSF surface after Al-Si removal (optical microscope), after firing a thick Al layer (12 mg/cm^2) at 900°C.

Cavities in dried aluminium paste

Thick aluminium layers need special care in the drying process (a slow heat-up ramp), because otherwise volatilizing solvents can build cavities in the paste. In figure 13 the cavities (13a) and the resulting unalloyed regions (13b) are correlated with the location of the screen mesh openings.

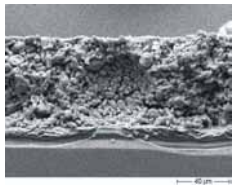

Figure 13a: 12 mg/cm2 Al-paste after firing, showing a spherical cavity and an unalloyed region below.

Figure 13b: Top view, after removal of the Al-Si. The unalloyed regions are visible as towers protruding from the surface.

7 ACKNOWLEDGEMENTS

The author gratefully acknowledges the financial support of the EU under project N° ENK6-CT-2001-00560 (EC2Contact) and would like to thank Gunnar Schubert, Bernhard Fischer and Barbara Terheiden for fruitful discussions.

8 REFERENCES

[1] J.L. Murray and A.J. McAlister, *Bulletin of Alloy Phase Diagrams* **5** (1984) 74
[2] L. Sarti *et al.,* Solar Cells **11** (1984) 51
[3] C.J.J. Tool *et al.,* 17th PVSEC Munich (2001) 1551
[4] V. Meemongkolkiat, *Colorado Workshop* (2004) 259